Indian Journal of Pure & Applied Physics
Vol. 61, March 2023, pp. 182-189 DOI: 10.56042/ijpap.v61i3.71028

Structural and Spectroscopic Properties of Eu^{3+} ions in Alumino-Silicate Glass

K M S Dawngliana[a*], A L Fanai[b] & S Rai[a]

[a]Laser and Photonics Laboratory, Department of Physics, Mizoram University, Aizawl 796 004, India

[b]Physic Section, Mahila Mahavidyalaya, Banaras Hindu University, Varanasi 221 005, India

Received 1 February 2023; accepted 27 February 2023

The structural, and optical properties of the Eu^{3+} ion in alumino-silicate $35Al(NO_3)_3$: (65-x) SiO_2 glass (x = 0.75, 2.0 and 4.0 mol%) were investigated. X-ray diffraction proved that the present glasses are amorphous. FTIR spectral analysis was used to determine which functional groups were present at specific annealing temperatures. The PL spectra with different Eu^{3+} concentrations are recorded with excitation wavelength 370 nmhave been recorded atroom temperature (RT). The PL spectra showed the ($^5D_0 \rightarrow {}^7F_J$; $J = 0....,4$) transitions of Eu^{3+} in the prepared glasses. The rise in Eu^{3+} ions in the host matrix was the explanation for the concentration quenching behaviour that was also seen. To ensure the dominant emission of the present glasses, the PL spectra were characterized using the CIE 1931 chromaticity diagram, and the results were discussed and reported in detail.

Keywords: Sol-gel; Europium; Aluminium; Photoluminescence; CIE chromaticity

1 Introduction

Glasses are ideal systems for photonic devices the study of their optical properties is an essential part of photonic devices. Rare-Earth (RE) ions doped in various host materials have been extensively studied over the years due to their potential in optoelectronics, bio-photonics, optical memory, and other fields[1-2]. There are many advantages to silica glass as a host for RE ions, these application-oriented studies of materials need optimized performance, which is hindered by the quenching mechanism. To avoid this quenching mechanism, effective dispersion of RE ions in the host is necessary. This dispersion of RE ions in silicate glass hosts is possible through the codoping of different metals and semiconductors such as Al_2O^3, etc. in the host lattice[3-6]. The formation of NBO (such as Al–O–RE[7], *etc.*) helps partition RE ions rather than clustering and forming RE–O–RE bonds[8]. The optical and physical properties of Eu^{3+}-doped silica glass by the sol-gel method have been extensively studied to study optical and physical properties in various hosts such as glass, powders, crystals, and so on[9-12]. Among these hosts, glass has gained lucrative interest due to its immediate device applicability[13]. The spectroscopic properties of RE ions are host independent due to their outermost shielding, although the phonon energy of a host is regarded as a deciding factor for optical performance[14]. The sol-gel technique is one of the preferable methods to prepare inorganic oxides and glasses of high purity and homogeneity for various optoelectronic and photonic applications due to its advantages of low-temperature processing, homogeneity, and low cost[15]. Theoretical and experimental work has been done on the spectroscopic properties of Eu^{3+} ions in the glass system[16]. The Eu^{3+} ion has the ground state J = 0, which induces a special restriction on the induced electric–dipole (ED) transitions originating from the ground state[17] and also has quite different luminescent intensities depending upon different symmetry sites[18]. Eu is widely utilized in commercial red luminous phosphors and is doped in silica glass. The electrons at the $^5D_0 \rightarrow {}^7F_2$ level's electric dipole transitions are what give the color red. It is hypersensitive to a local symmetry, in other words, lattice plays an important role in its PL, thus making Eu^{3+} an ideal candidate to investigate the dependence of glass compositions on luminescence characteristics.

In this paper, we investigate the structural, and spectroscopic properties of (0.75, 2.0, and 4.0 mol%) of Eu^{3+} ions in the alumino-silicate glass.

2 Experimental Procedures

The glasses containing Eu^{3+} in (65-x) SiO_2:$35Al(NO_3)_3$:xEu_2O_3 (where x = 0.75, 2.0, or 4.0 mol%) were made using a sol-gel technique.

*Corresponding authors:
(E-mail: jerrykms0000@gmail.com)

Methanol is used as a solvent, Nitric acid (HNO_3) as the catalyst, and Tetraethyl orthosilicate (TEOS) is used as the main precursor. $Eu_2O_3$is used as the source for Eu^{3+} ions. The dopant is mixed with banana trunk sap, methanol, and nitric acid. The solution is stirred for 40 min. To this solution, TEOS is added and further stirred for 2 hours using a magnetic stirrer to form a sol. The molar ratio of TEOS, nitric acid, banana trunk sap, and methanol is 16:4:10:70. The resulting sol is then poured into a plastic container, sealed, and kept from evaporating. Pinholes are made in the lid of a plastic container to allow for slow evaporation after the sol has solidified into a gel after being sealed at room temperature for 24 days. The container is then left for a few weeks. The gels are further dried by slowly heating to 50 °C and then annealing up to 1050 °C at a heating rate of 1 °C/min in an electric muffle furnace to create dense glass samples in the form of discs. The Abbe refractometer method was used to calculate the refractive index.

The absorption and photoluminescence spectra of the glass samples were recorded using an iHR320 imaging spectrometer. A diffractometer (Panalytical Empyrean) was used to record XRD patterns using CuKα (λ_{ex}= 1.54Å) radiation. FTIR spectra were recorded by IRAffinity-1S (SHIMADZU). Glass densities were measured using acetone as an immersion liquid from Archimedes' principle. With an accuracy of (n± 0.001), the refractive index of the transparent present glasses was calculated using an Abbe refractometer with a coating of 1-bromonaphthalene (C10H7Br). All the spectra were recorded at RT.

3 Results and Discussion

3.1 XRD Spectra

Fig. 1 shows the (2.0 mol%)Eu^{3+} ions co-doped alumino-silicate glass' powdered XRD spectrum after being annealed at 900 °C.The distinct broad hollow peaks around 2θ = 22° are observed rather than intense crystalline peaks with a crystallinity index of more than 39%, which established the glassy amorphous nature of the prepared sample[19].

3.2 FTIR Spectra

Figure 2 shows the FTIR spectra of the co-doped (2.0 mol%) Eu^{3+} ions in aluminum-silicate glass that were annealed at 600 °C and 950 °C, respectively. These spectra were recorded in the 400–4000 cm^{-1} range. The various peak positions and vibrations

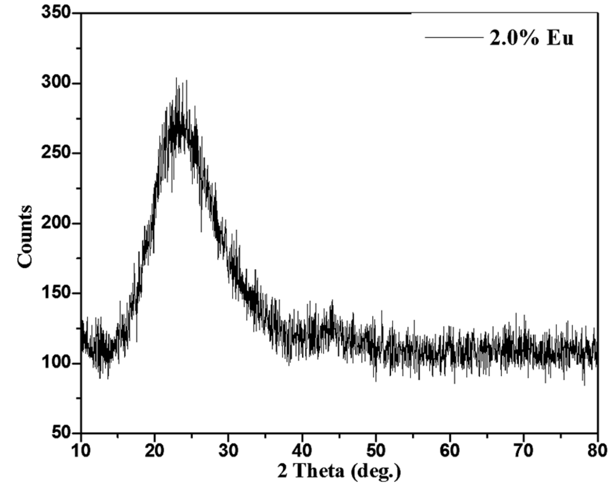

Fig.1 — XRD of co-doped Eu^{3+} (2.0 mol%) in aluminum-silicate glass that was annealed at 900 °C.

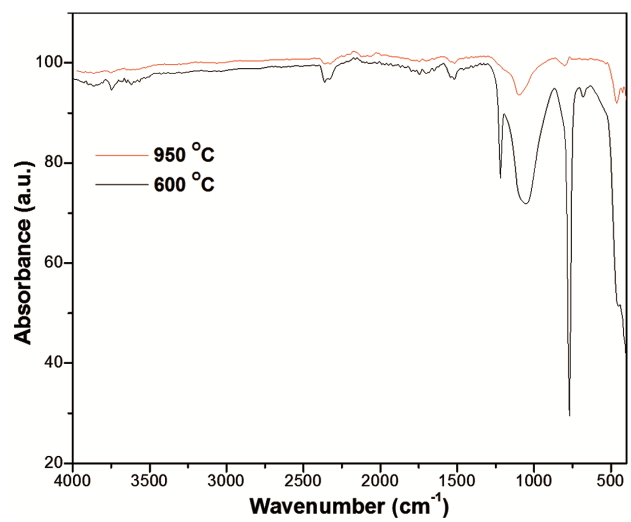

Fig. 2 — FTIR spectra of glass co-doped with Eu^{3+} ions (2.0 mol%) at various annealing temperatures.

assigned are shown in Table 1. The samples in the gel stage have a lot of H_2O and other organics. The slow heating of the prepared sample in an electric muffle furnace leads to the gradual reduction of various compounds from the gel matrix and contributes to the formation of a rigid glassy network. Due to the polymerization process of symmetric stretching of Si-O-Si or vibrational modes of the ring structure, respectively, a weak band at around 772 cm^{-1} is observed for the gel annealed at 600 °C. A sensitive peak around 1215 cm^{-1} is owing to vibrations of TEOS, an ethoxy group. The Eu^{3+} ions doped in the glass matrix contribute to the peaks at around 1042–1093 cm^{-1}. The vibrations due to the deformation of the bonds of the H_2O molecules are

Table 1 — The glass sample's FTIR peak positions and various assignments.

Wavenumber (cm^{-1})	Assignment	Observed intensity	Change in intensity during heating
444-452	Vibrations of asymmetric stretching in Si-O, O-Si-O stretching[20]	Minor	A minor peak arises at 600 °C, Intense peak arises at 950 °C.
686	Vibration of asymmetric Si-O-Al bending with NBO (non-bridging oxygen)[21]	Intense peak	At 600 °C, intense peaks appear, and they disappear at 950 °C.
763-791	Si-OH stretching[20]	Strong	Decrease when the temperature rises
1042-1093	Si-O-Al, asymmetric stretching[20]	Strong	Redshift, decrease in intensity
1215	C-O-C stretching vibration[22]	Minor peak	Remove in T >950 °C
1525	–OH bending vibration mode of water	Strong	At increasing temperatures peak will be decreased
2365	Deformation of the water molecules' bonds through vibrations[23]	Minor peak	Decrease with increasing temperature
3700-3748	O-H stretching[20]	Broad	In T > 950 °C, it is fully removed.

Table 2 — Certain physical properties ofEu^{3+}co-doped with Al in sol-gelSiO_2 glasses.

Physical properties	Eu(0.75%)	Eu (2.0%)	Eu (4.0%)
Refractive index (n)	1.643	1.647	1.649
Density (ρ) (gcm^{-3})	2.102	2.204	2.301
Thickness (Z)	0.215	0.219	0.227
Average molecular weight M_T (g)	75.82	77.66	80.58
Eu^{3+} ions concentration (N_i)($x10^{20}$)	1.252	2.903	6.876
Dielectric constant (ε)	2.699	2.713	2.719
Optical dielectric constant (P dt/dp)	1.699	1.713	1.719
Molar volume (V_m) (cm^3/mol)	36.07	35.24	35.02
Reflection loss (R_L)	0.059	0.060	0.060
Molar refraction (R_M)	13.042	12.808	12.757
Energy gap (E_g)	8.14	8.12	8.08
Polaron radius r_p(Å)	8.05	6.09	4.57
Inter nuclear distance (r_i)($x10^{-7}cm^{-3}$)	2.93	2.21	1.66
Electronic polarizability (α_e)(x 10^{21})	1.43	1.44	1.45
Field strength (F)(x 10^{13} cm^{-2})	3.318	5.905	10.869
Molar polarizability (α_m)	5.175	5.083	5.062
Oxygen packing density (OPD)	36.151	35.782	33.561
Metallization criterion (M)	0.638	0.637	0.636

related to the peaks around 2365 cm^{-1}. Si-O-Si bending modes are ascribed to the peaks about 678 cm^{-1}. Then, the bending mode of H_2O molecules is assigned to the other weak bands at about 3700–3748 cm^{-1}. Thus, FTIR spectra of Eu^{3+} doped in alumino-silicate glass confirm the invariance of the silica matrix structure with Eu^{3+} doping and annealing temperature.

3.3 Physical Properties of Eu^{3+} Doped in Al-Si Glass

Certain physical properties have been estimated from the measured glass densities, refractive index for all this Eu^{3+} doped glasses. These values are presented in Table 2. These values are estimated using the method described in our earlier paper[24].

3.4 Absorption Spectra

Figure 3 shows the absorption spectra of Eu^{3+} ions in SiO_2 sol-gel glass with fixed aluminium. In the UV-VIS range (355-480 nm), absorption bands resolved correspond to the transitions $^7F_0 \rightarrow {}^5D_4$ (362 nm), $^7F_0 \rightarrow {}^5G_4$ (375 nm), $^7F_0 \rightarrow {}^5G_2$ (379 nm), $^7F_0 \rightarrow {}^5G_3$ (385 nm), $^7F_0 \rightarrow {}^5L_6$ (394 nm), and $^7F_0 \rightarrow {}^5D_2$ (465 nm).The data of Carnal et al. is used to assign all above peaks[25]. The $^7F_0 \rightarrow {}^5D_2$ induced electric-dipole transition is hypersensitive in nature and is known to exhibit wide variation in its band intensity[26]. The strongest absorption band in the glass is the transition band between $^7F_0 \rightarrow {}^5L_6$. The transition ($^7F_0 \rightarrow {}^5L_6$) is allowed by the ΔJ rule even if it is prohibited by the ΔS and ΔL selection rules.

3.5 Photoluminescence Spectra

The PL spectra of the Eu^{3+} (0.75, 2.0, and 4.0 mol%) ions co-doped with a fixed aluminium concentration in sol-gel silica glasses are shown in Fig. 4. A 370 nm source is used to excite the Eu^{3+} ions from their ground state of $^7F_0$ to their excited state

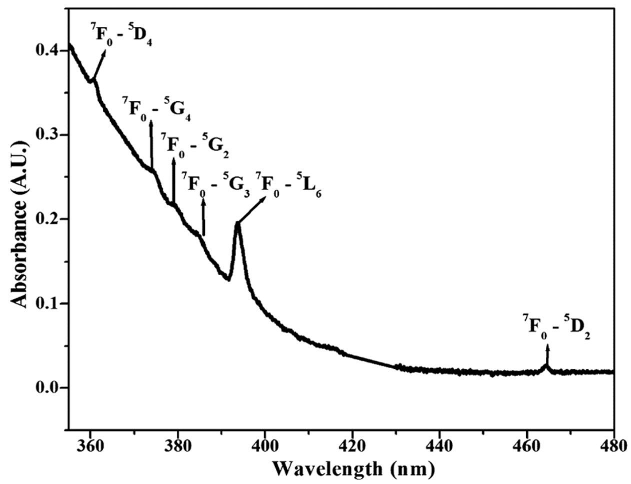

Fig. 3 — Absorption spectra of (2.0 mol%)Eu^{3+} ions co-doped with Al sol-gel silica glasses.

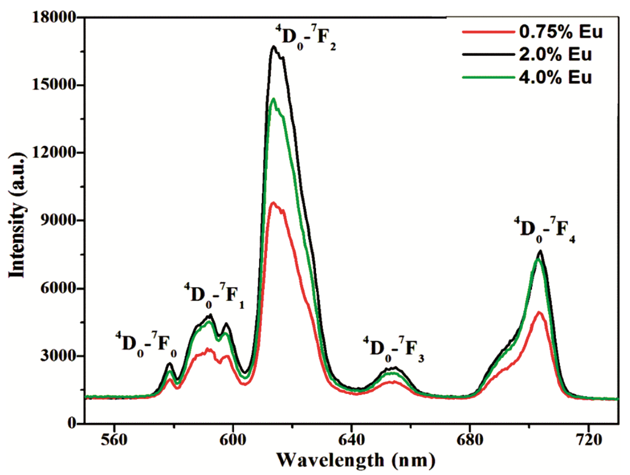

Fig. 4 — PL spectra of Eu^{3+}ions co-doped with Alsol-gel silica glasses.

of $^5D_2$.The emission spectra consist of five groups of emission bands at around 578, 592, 614, 654, and 703 nm, which result from the transitions $^5D_0 \rightarrow {}^7F_J$ (J = 0, 1, 2, 3, and 4), respectively[27]. Fluorescence intensity varies with concentrations of Eu^{3+}, the fluorescence intensity is maximum for 2 mol% of Eu^{3+}. But it is decrease at high concentration 4 mol%. It indicate that the formation of clusters at higher concentrations of Eu^{3+}, due to which fluorescence quenching occurs.

The line emissions in the spectra correspond to $^5D_0 \rightarrow {}^7F_0$ (578 nm), $^5D_0 \rightarrow {}^7F_1$ (592 nm), $^5D_0 \rightarrow {}^7F_2$ (614 nm), $^5D_0 \rightarrow {}^7F_3$ (654 nm) and $^5D_0 \rightarrow {}^7F_4$ (703 nm) transitions of Eu^{3+} ions[27-29]. Because there is no crystal field splitting at the $^5D_0$ and $^5F_0$ levels, the $^5D_0 \rightarrow {}^7F_0$ transition is also useful for determining the bonding environment of the Eu^{3+} ions. All of the glass samples

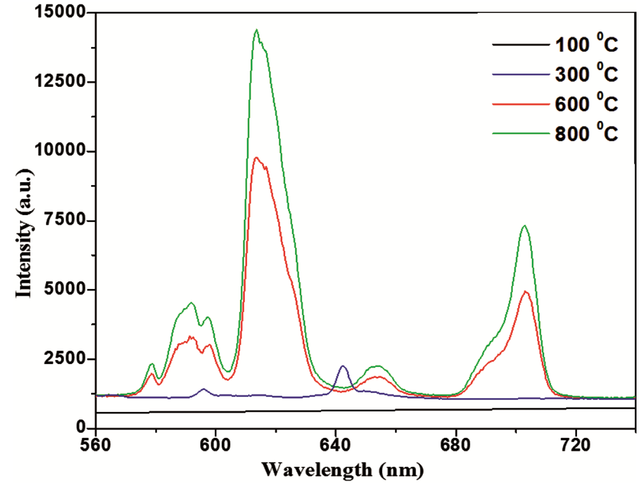

Fig. 5 — Effect of annealing temperature on PL intensity. (Note: PL intensities of samples annealed to 100 °C and 300 °C are magnified to 100 and 10 times for clarification).

with various amounts of Eu^{3+} had a relatively low peak at 578 nm. The $^5D_0 \rightarrow {}^7F_2$. Is an electric dipole allowed transition and its intensity is hypersensitive to the variation of the bonding environment of theEu^{3+}ions, while $^5D_0 \rightarrow {}^7F_1$ is a magnetic dipole allowed transition and its intensity hardly varies with the bonding environment of theEu^{3+} ions[30,31]. The strong emission peak at 614 nm is shown in Fig. 4, which can be attributed to the hypersensitive ED transition. It is established that the Eu^{3+} ion is located at low-symmetry sites because the intensity of emission of the ED transition is significantly higher than intensity of the MD transition. With the increase in Eu^{3+} ions concentrations, a relative change in the intensities of the emission peaks is also seen.

3.6 Annealing Temperature's Effect on PL Spectrum

The PL spectra of Eu^{3+} (2.0 mol %) ions co-doped with a fixed aluminium concentration in sol-gel silica glasses were annealed at different annealing temperatures (100, 300, 600, and 800 °C) as shown in Fig. 5. The sample quenched by the hydroxyl (OH) group exhibits very little intensity after being annealed at 100–300 °C. The PL of Eu^{3+} ions has been quenched by the high phonon energy of the OH group. In silica xerogel, energy release and transfer to the Eu^{3+} ions is suppressed by the generation of electrons and holes from the recombination of defects. For higher temperatures were used to anneal the sample, the rise of asymmetry caused by the growth of NBO (Si-O-Al), which has a lower phonon energy than the vibration of the Si-O-Si bond, contributes to PL enhancement. This is already confirmed from recorded FTIR spectra. Thus, the PL intensity increases for dense glasses that are annealed at higher temperatures after the OH group is removed (Fig. 5). As a result, PL enhancement is successfully accomplished by asymmetry in the host matrix and OH group removal at a high annealing temperature.

Fig. 6. Shows schematic energy level diagram of allowed transition levels for Eu^{3+} ions involved in emission process.

3.7 Absorption Spectra and Judd-Ofelt Analysis

Quantitative analysis of several *f-f* transitions of Eu^{3+} (2.0 mol%) co-doped with fixed aluminium in sol-gel SiO_2 glasses is calculated using the Judd-Ofelt (JO) theory (Fig. 3).The JO parameters[32,33] are estimated to extract practical information regarding the different optical properties and the Eu^{3+} ion's neighborhood in the aluminiumco-doped silica host. The three JO parameters [Ω_λ] determine the oscillator strengths (f_{cal}) derived from each absorption peak as a result of transitions $|\Psi J\rangle \rightarrow |\Psi' J'\rangle$, and they have the following expression:

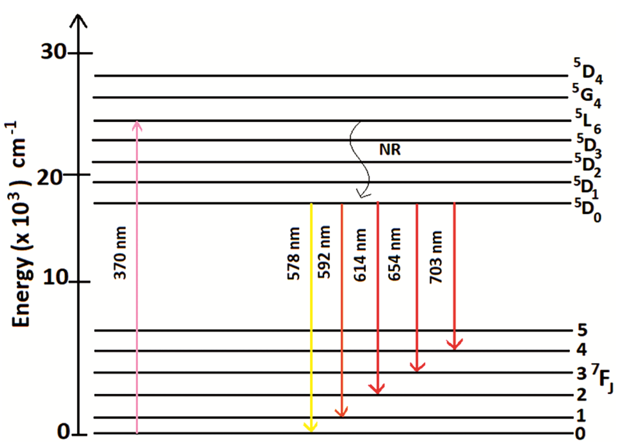

Fig. 6 — Energy diagram of co-doped Eu^{3+} and Al ions in a silica host schematic.

$$f_{cal}^{ed} = \frac{8\pi^2 m_e c\bar{\upsilon}(n^2+2)^2}{3h(2J+1)9n} \Sigma_{\lambda=2,4,6}\Omega_\lambda(\Psi J\|U^\lambda\|\Psi' J')^2 \quad \ldots(2)$$

Where m_e is mass of electron, h is the Planck's constant, c is the vacuum speed of light, $n_i$is the index of refraction, and J is the ground state of total angular momentum, $\|U_\lambda\|$ are the doubly reduced matrix elements [RME] evaluated in the intermediate coupling approximation for a transition $\|\Psi J\rangle \rightarrow |\Psi' J'\rangle$ at energy $\bar{\upsilon}$ expressed in cm^{-1}.The host independent RME values, $\|U^\lambda\|$ are used in this calculation as obtained by Carnal *et al.*[34].

The intensities of the absorption bands or experimental oscillator strengths (f_{exp}) are calculated using relation

$$f_{exp} = 4.319 \times 10^{-9} \int \varepsilon(\bar{\upsilon})dv \quad \ldots(3)$$

Molar absorptivity with wave number (in cm^{-1}) is represented by the symbol $\varepsilon(\bar{\upsilon})$.With the use of MATLAB (MATLABR12) commands, at the proper stage, the {solution to the correlation matrix} for forced electronic dipole transitions is obtained. The f_{exp} and f_{cal} are correlated, which was determined from the aforementioned Eq. (3) and from Eq. 2, is fitted using least squares to estimate the JO parameters. The RME estimated in Carnal *et al.*[35] and index of refraction (n=1.647) of 2.0 mol% Eu^{3+} and fixed aluminium co-doped silica glass was used in these calculations and as cited in Table 3. The pattern in JO parameter has been identified as ($\Omega_4 > \Omega_2 > \Omega_6$). The large value of Ω_4 reasonably specifies the existence of covalent bonding among Eu^{3+} ions and other two metals in host [Eu-O, Eu-Al][36,37]. Here Ω_2 is extremely structure sensitive and association with the symmetry and covalency of the Eu^{3+} ions neighborhood[38]. The values of Ω_4 and Ω_6 are decided by the viscosity and dielectric properties of the media (glass) and induce vibronic transition due to the

Table 3 — The oscillator strengths for fixed Al and Eu^{3+} (2.0 mol%) co-doped sol-gel SiO_2glass after 1050 °C annealing, as calculated (f_{cal}) and experimentally (f_{exp}).

Transitions	Energy (in cm^{-1})	Wavelength (in nm)	f_{exp} (x 10^{-6})	f_{cal} (x 10^{-6})
$^7F_0 \rightarrow {}^5D_4$	27624	362	0.121	0.183
$^7F_0 \rightarrow {}^5G_4$	26667	375	0.214	0.113
$^7F_0 \rightarrow {}^5G_2$	26385	379	0.087	0.093
$^7F_0 \rightarrow {}^5G_3$	25974	385	0.072	0
$^7F_0 \rightarrow {}^5L_6$	25381	394	1.173	1.173
$^7F_0 \rightarrow {}^5D_2$	21505	465	0.107	0.101
Ω_2=3.346±0.031 (x 10^{-20} cm^2)	Ω_4= 3.428± 0.013 (x 10^{-20} cm^2)	Ω_6=1.695±0.046 (x $10^{-20}cm^2$)		
		Ω_4/Ω_6 =2.022 ± 0.063 (x 10^{-20})		

Table 4 — Judd Ofelt intensity metrics compared for Eu^{3+} doped in different hosts.

Ω_2	Ω_4	Ω_6	Ω_4/Ω_6	References
3.346	3.428	1.695	2.022	Present work
0.64	4.87	2.84	1.71	ZBLA [36]
5.44	4.44	5.38	0.83	L5FBE [41]
11.62	-	2.82	-	L4BE [41]
5.61	3.47	2.91	1.19	$Al(NO_3)_3$-SiO_2 [42]
6.36	3.94	0.51	7.73	KMgSi [43]
5.47	1.55	1.07	1.45	BaO [44]

Table 5 — Radiative lifetime (τ), branching ratio (βr (%)), total transition probability (A_S), and probability of radiative transitions (A_{ed}) for the emission transition of Eu^{3+} (2.0 mol%) co-doped with fixed aluminium in sol-gel SiO_2 glasses.

Transitions	Energy (in cm^{-1})	A_{ed} (in s^{-1})	β_r (in %)	λ_{eff} (nm)	σ_P (x $10^{-22}cm^2$)
$^5D_0 \rightarrow {}^7F_0$	17301.038	0	0	2.075	0
$^5D_0 \rightarrow {}^7F_1$	16891.892	63.732	14.609	12.605	2.702
$^5D_0 \rightarrow {}^7F_2$	16286.645	271.157	62.156	14.410	11.638
$^5D_0 \rightarrow {}^7F_3$	15290.520	0	0	10.761	0
$^5D_0 \rightarrow {}^7F_4$	14244.751	101.362	23.235	13.085	8.233

A_T (s^{-1}) = 436.251 τ_R= 2.292 (ms)

Table 6 — CIE chromaticity coordinates of Eu^{3+} (0.75, 2.0, 4.0 mol%) in sol-gel silicate glasses co-doped with Al.

Color Coordinates	Eu (0.75mol%)	Eu (2.0mol%)	Eu (4.0mol%)
X	0.502	0.544	0.529
Y	0.382	0.371	0.377

bond between Eu^{3+} ions and the ligand atoms[39]. The spectroscopic quality (Ω_4/Ω_6) is significant in foreseeing the stimulation of emission for the laser active host[40]. Table 4 shows the comparisons of the JO intensity parameters of Eu^{3+} doped glasses.

3.8 Radiative Properties

The measured PL spectra of the fluorescence level $^5D_0$ of the Eu^{3+} (2.0 mol%) co-doped with fixed aluminium in SiO_2 sol-gel glasses and the absorption spectra of the corresponding fluorescence level are combined to provide the phenomenological parameters known as the JO intensity parameters. Finally the emission cross-section of peaks [$\sigma_P(\lambda_P)$] among initial (ΨJ) and a terminal manifold ($\Psi' J'$) are calculated from[45]

$$\sigma_P(\lambda_P) = \frac{\lambda_P^4}{8\pi c n^2 \Delta\lambda_{eff}} A(\Psi J;\ \Psi' J') \quad ...(4)$$

Here λ_P stand for peak emission wavelength, $\Delta\lambda_{eff} = \frac{\int I(\lambda) d\lambda}{I_{max}}$ is the effective bandwidth, n stand for index of refraction and $A(\Psi J;\Psi' J')$ stand for probability of emission for the particular transition estimated from Table 5. The electric-dipole probability is the only factor considered in the computation of the probability of a radiative transition between the state (ΨJ) and (Ψ′J′), tis given as

$$A_{ed}(\Psi J;\Psi' J') = \frac{64\pi^4 e^2 n(n^2+2)^2}{3h\lambda^3(2J+1)9} \Sigma_{\lambda=2,4,6} \Omega_\lambda (\Psi J \| U^\lambda \| \Psi' J')^2 \quad ...(5)$$

Where ƛ is the transition of average wavelength.

Calculations for the fluorescence branching ratios include,

$$\beta_r = \frac{A(\Psi J;\Psi' J')}{\sum A(\Psi J;\Psi' J')} \quad ...(6)$$

And is used to predict the relative intensity of a line originating from a specific excited state.

The formula to calculate the radiative lifetime of an excited state *(ΨJ)*is as follows.

$$\tau_R = \frac{1}{\Sigma A(\Psi J;\Psi' J')} \quad ...(7)$$

The radiative parameters of the dense glass sample are calculated using these equations and are shown in Table 5 below.

3.9CIE Chromaticity

The PL emission of Eu^{3+} (0.75, 2.0, and 4.0 mol%) ions co-doped with a fixed aluminium concentration in sol-gel silica glasses has been exemplified using the CIE 1931 chromaticity Fig 7. The sample's estimated color chromaticity coordinates, CIE X and CIE Y, are listed in Table 6. Color tunability of PL spectra from Orange to Red is evident

Table 7 — Sol-gel alumino-silicate glass was doped with different nonlinear levels of Eu^{3+} (2.0 mol%) and annealed at 950 °C.

n_F	n_r	n_F–n_r	n_b	υ_{Ab}	$1/\upsilon_{Ab}$	n_2 (in 10^{-13} esu)	γ_{ce} (in cm^2/W)	ω_o x 10^{-13}	N x 10^{-16}	$\chi^{e(3)}$ x 10^{-6}
1.628	1.616	0.012	1.622	51.833	0.019	1.834	0.473	113.238	1085.966	2.396

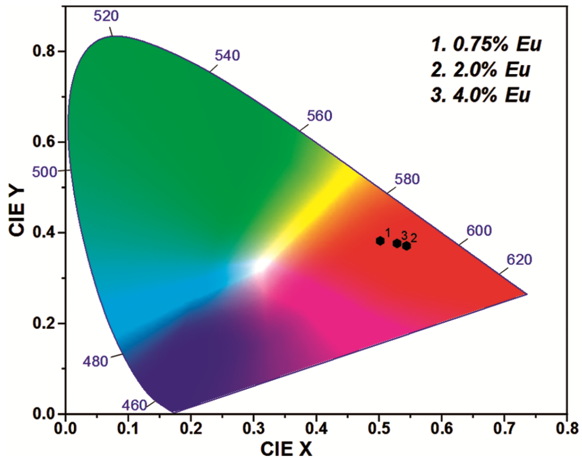

Fig. 7 — CIE chromaticity of Eu^{3+} ions co-doped with Al sol-gel glasses at different Eu^{3+}concentrations.

with Eu^{3+} concentrations quenching occurs as shown in Fig. 7.

4.0 Non-Linear Propertiesof Eu^{3+} Doped in Al-Si Glass

Certain non-linear properties have been estimated from optical parameters like the non-linear refractive index (n_2), non-linear refractive index susceptibility ($\chi^{e(3)}$),co-efficient (γ_{ce}), and reasonably high Abbe number (υ_{Ab}) indicate the good optical quality of the sol-gel SiO_2glass.These values are presented in Table 7. These values are estimated using the method described in our earlier paper[46].

5 Conclusions

The Sol-Gel method was used to successfully synthesis the Eu^{3+} (0.75, 2.0, and 4.0 mol%) doped in the alumino-silicate glass. The transparent glass samples are of good optical quality. The XRD spectra confirmed that the glass samples were amorphous. The FTIR spectra analysis confirms the removal of the OH-group along with the formation of NBO. The PL spectral is confirmation of the utility of prepared materials in optoelectronic devices. The chromaticity diagram is evidence of color tunability at different Eu^{3+} ion concentrations.

Additionally, the high optical quality of the glass as well as its excellent third-order non-linear behaviour are confirmed by the physical and non-linear properties, such as the relatively high Abbe number (υ_{Ab}),low non-linear refractive index (n_2), co-efficient (γ_{ce}) and susceptibility ($\chi^{e(3)}$) values.

Acknowledgements

KMS Dawngliana is thankful to university Grants Commission, India for UGC-MZU (Non-NET) fellowship, for financial support with Award letter No.12-1/MZU (Acad)/21/405.

Conflicts of Interest

The authors declare no conflict of interest.

Reference

1 Arai K, Namikawa H, Kumata K, Honda T, Ishii Y & Handa T, *J Appl Phys*, 59 (1986) 3430.
2 Wang J, Brocklesby W S, Lincoln J R, Townsend J E & Payne D N, J Non-Cryst Solids, 163 (1993) 261.
3 Lochhead M J & Bray K L, *Chem Mater*, 7 (1995) 572.
4 Stone B T & Bray K L, *J Non-Cryst Solids*, 197 (1996) 136.
5 Tanabe S & Hanada T, J Non-Cryst Solids, 196 (1996) 101.
6 Chiasera A, Montagna M & Rolli R, *J Sol–Gel Sci Technol*, 26 (2003) 943.
7 Monteil A, Chaussedent S & Alombert G S, *J Non-Cryst Solids*, 348 (2004) 44.
8 Alombert G G, Gaumer N, Obriot J & Rammal A, *J Non-Crystal Sol*, 351 (2005) 1754.
9 Hench L L & West J K, *Chem Rev*, 90 (1990) 33.
10 Brinker C J & Scherer G W, Sol-Gel Science: *The Physics and Chemistry of Sol-Gel Processing*, Academic Press, New York, 1990.
11 Collings B C & Silversmith A J, *J Lumin*, 62 (1994) 271.
12 Hreniak D, Jasiorski M, Maruszewski K, Kepinski L, Krajczyk L, Misiewicz J & Strek W, *J Non-Crystalline Solids*, 298 (2002) 146.
13 Rai S & Fanai A L, Optical spectroscopic properties of Nd^{3+} ions in aluminum glass matrix, National Laser Symposium (NLS-24), RRCAT, Indore, 2015.
14 Fan X, Wang M & Xiong G, *Spectroscopic studies of RE ions in silica glasses prepared by the sol-gel process*, 27 (1996) 177.
15 Martinez J R & Erika E, *New J Glass Ceram*, 1 (2011) 7.
16 Swapna K & Mahamuda S K, *J Lumin*, 146 (2014) 288.
17 Wong P S & Wan M H, *J Rare Earths*, 32 (2014) 585.
18 Lee S H, Du P, Bharat L K & Yu J S, *Ceram Int J*, 43 (2017) 4599.
19 Wang S S, Zhou Y, Lam Y L, Kam C H, Chan Y C & Tao X, *Mat Res Innov*, 1 (1997) 92.
20 Jiao Y, Guo M, Wang R, Shao C & Hu L, *J Appl Phys*, 129 (2021) 053104.
21 Kumar N K, Vijayalakshmi L & Ratnakaram Y C, *Opt Mater*, 45 (2015) 148.
22 Driss L, Behilil A & Zahraoui B, *Environ Prog Sustain Energy*, 38 (2019) 1.
23 Umar S A, Halimah M K, Chan K T & Latif A A, *J Non-Crystal Sol*, 471 (2017) 101.
24 Dawngliana K M S, Lalruatpuia, Fanai A L & Rai S, Mater Today, 65 (2022) 2572.

25 Carnal W T, Fields P R & Rajnak K, *J Chem Phys*, 49 (1968) 442.
26 Hazarika S & Rai S, *Opt Mater*, 27 (2004) 173.
27 You H & Nogam M, *J Phys Chem B*, 108 (2004) 12003.
28 Manju G R J, Gopi S, Mathew S S, Saritha A C & Biju P R, *RSC Adv*, 10 (2020) 20057.
29 Binnemans K, *Chem Rev*, 295 (2015) 1.
30 Chang M, Song Y, Sheng Y, Chen J & Zou H, *Phys Chem Chem Phys*, 19 (2017) 17063.
31 Kostova I, Patronov G & Tonchev D, *J Chem Technol Metal*, 53 (2018) 1087.
32 Judd B R, *Phys Rev*, 127 (1962) 750.
33 Ofelt G S, *J Chem Phys*, 37 (1962) 511.
34 Carnall W T, Crosswhite H & Crosswhite H M, Energy level structure and transition probabilities in the spectra of the trivalent lanthanides in LaF_3, Argonne National Laboratory, Report no. ANL-78-XX-95, 1978.
35 Carnall W T, Fields P R & Rajnak K J, *Chem Phys*, 59 (1968) 4424.
36 Dejneka M, Snitzer E & Riman R E, *J Lumin*, 65 (1995) 227.
37 Hazarika S & Rai S, *Proc 6th International Conference on Optoelectronics*, Fibre Optics and Photonics, Mumbai, 2002.
38 Vijayakumar M, Marimuthu K & Sudarsan V, *J Alloys Compd*, 647 (2015) 209.
39 Khan U, Fanai A L & Rai S, *Adv Eng Res*, 178 (2018) 194.
40 Agarwal A, Pal I, Sanghi S & Aggarwal M P, *Opt Mater*, 32 (2009) 339.
41 Babu P & Jayasankar C K, *Physica B*, 279 (2000) 262.
42 Hazarika S & Rai S, *Opt Mater*, 27 (2004) 173.
43 Nageno Y, Takebe H, Morinaga K & Inzumitani T, *J Non-Cryst Solids*, 169 (1994) 288.
44 Tripathi G, Kumar R V & Rai S B, *Opt Commun*, 264 (2006) 116.
45 Chamarro M A, Cases R & Aleala R, *Ann de Physique*, 16 (1991) 227.
46 Dawngliana K M S & Rai S, *J Non-Crystal Sol*, 598 (2022) 121929.